ISSN 2616-5775 Vol. 7, Issue 5: 159-167, DOI: 10.25236/AJCIS.2024.070521

Investigation on Visual Computing Model of Mathematics Educational Resources Based on Image Processing Technology

Chengxiu Dong

Department of Primary Education, Jinan Preschool Education College, Jinan, Shandong, 250307, China
393860282@qq.com

Abstract: *In order to formulate a scientific teaching resource management method, this paper proposed a research on the visual computing model of mathematical educational resources based on image processing technology. In this paper, a shared learning model based on cloud computing was constructed through HOG feature extraction, and an image denoising method was used to simplify the algorithm, and the Fast R-CNN model algorithm was improved accordingly. The improved visual computing model could directly add bounding box regression to the CNN network for training. In the experiment, the comparison test of processing speed with different number of nodes was carried out, and the performance test was carried out by applying the improved Fast R-CNN model algorithm. The experimental results showed that the 1126.4MB data packet took 36s before the improvement, the 2355.2MB data packet took 41s, the 1126.4MB data packet took 20s, and the 2355.2MB data packet took 22s. It indicated that using this improved algorithm could improve the access speed and data processing performance of the storage model.*

Keywords: *Image Processing, Mathematics Educational Resources, Visual Computing Model, Fast R-CNN Model Algorithm*

1. Introduction

Traditional teaching resource storage has been difficult to meet the growing demand for data storage. Therefore, colleges and universities are faced with the serious problems of scattered teaching resources, low resource utilization, and high resource maintenance costs. In the past, most colleges and universities used central servers to store this data. However, as this data continues to evolve, the cost of colleges and universities to store large amounts of educational resources and the difficulty of board work will continue to increase. At the same time, it will lead to repeated adjustment of hardware resources and waste a lot of infrastructure resources. Therefore, an important and urgent problem faced by colleges and universities in the development of educational informatization is the storage method, efficient and low-cost management and use of a large number of teaching resources.

In the visualization of educational resources, Amabili L et al. based on constructivism and the concept of learning by playing, proposed a dual model for designing visual educational games: a construction game and a structure game. Both games use the same deck of cards, are simple in design, and are popular in visualization teaching [1]. Uranova V V et al. studied the role of visual information in the medical biology education of students, and the experimental results proved that the use of visual materials performed well in the success rate and quality indicators of the student group, and the visual concepts and algorithms created by the experiment could be used as teaching materials [2]. Zhang C et al. evaluated the educational effect of stereoscopic augmented reality (AR) visualization and the modification effect of visuospatial ability on learning, and the experimental results proved that this technology can significantly help students with low visuospatial ability in anatomy teaching [3]. Fatemah A et al. proposed a technical solution that successfully helped students improve their spatial learning process by creating a link between two-dimensional representations of chemical structures and three-dimensional molecular visualization in real time [4]. Experimental results showed that this method could effectively narrow the performance differences among students with different spatial ability levels.

In image processing, Ghamisi P et al. based on mathematical morphology and other disciplines,

ISSN 2616-5775 Vol. 7, Issue 5: 159-167, DOI: 10.25236/AJCIS.2024.070521

using spectral and spatial information, the hyperspectral image classification technology has undergone revolutionary changes [5]. Hsieh M C et al developed an interactive intelligent augmented reality teaching system for mathematics teaching, which consists of learning AIDS, virtual tutors and mathematical problem solving guidance mechanisms [6]. The experimental results discuss the significance of using augmented reality for teaching and learning. Ruthotto L et al. established a new partial differential equation interpretation for a class of deep convolutional neural networks commonly used to learn from speech, image, and video data, resulting in two new classes of convolutional residual neural network structures: parabola and hyperbola [7]. The results can help people understand mathematics. Hidayati D Wet al. explored the relationship between self-regulated learning and mathematical critical thinking ability. By using GeoGebra software to teach 3D geometry, students' critical thinking can be stimulated, including the practice of information collection, independent spatial ability, and the ability of interpretation, analysis, evaluation and reasoning in self-regulated learning [8].

With the continuous development of science, image matching technology plays an increasingly important role in many fields. Image matching is not only widely used in scientific research, but also widely used in daily life. The current research mainly focuses on the accuracy, speed and anti-interference of image matching to improve the effect of image matching [9].

2. Construction Method of Visual Computing Model of Mathematics Educational Resources

2.1 HOG Feature Extraction

For targets with simple geometric features, the edge of the target is mainly obtained by edge detection, and then features such as lines and circles are extracted to achieve target detection. However, when encountering object detection states with complex geometric features, it is difficult to obtain relatively complete edges from edge detection [10]. At present, the effect of using the methods for object detection is not ideal [11]. Besides the obvious geometric features, the pixel distributions on the target and the background are different, thus resulting in a large difference in texture between the target and the background [12]. Pattern matching algorithms are common object detection algorithms based on this difference. Template matching algorithms locate sub-image detection windows in an image that are more similar to the template image by directly comparing the pixel differences between the template image and its image [13]. Image grading information reflects the grayscale variation of pixels in spatial image sectors [14]. This object detection algorithm can reduce the effects of illumination changes and has good durability [15]. The HOG feature extraction process is shown in Figure 1:

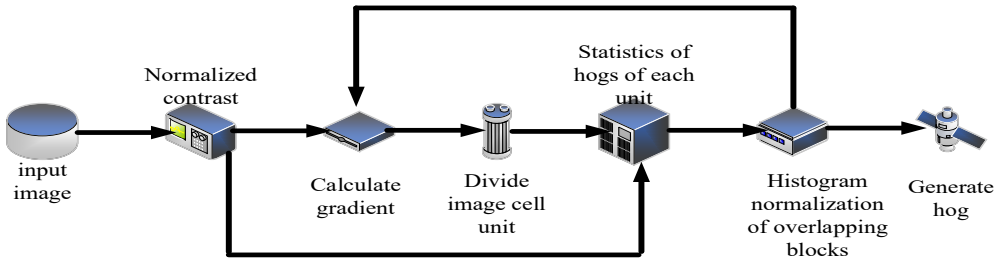

Figure 1: HOG feature extraction process

The tilt range and direction of each pixel are calculated. The direction of the gradient represents the direction of the maximum rate of change of the grayscale image at this time, and the range of the gradient represents the maximum rate of change. In order to reduce the influence of noise, the image is smoothed using a standard before calculating the slope, but this processing will weaken the response of the edge, so choosing an appropriate variance is very important for the final detection result. In addition, different rating operators can also affect the detection results.

2.2 Shared Learning Model Based on Cloud Computing

In the daily learning process, the reliance on the computing cloud is beneficial to facilitate collaborative learning. The design of educational behavior in the computing cloud environment can be divided into three stages: The first stage is to clarify the project and think independently. The second stage is collaborative communication and peer evaluation. The third stage is to monitor performance

ISSN 2616-5775 Vol. 7, Issue 5: 159-167, DOI: 10.25236/AJCIS.2024.070521

and reflect on evaluation, as shown in Figure 2.

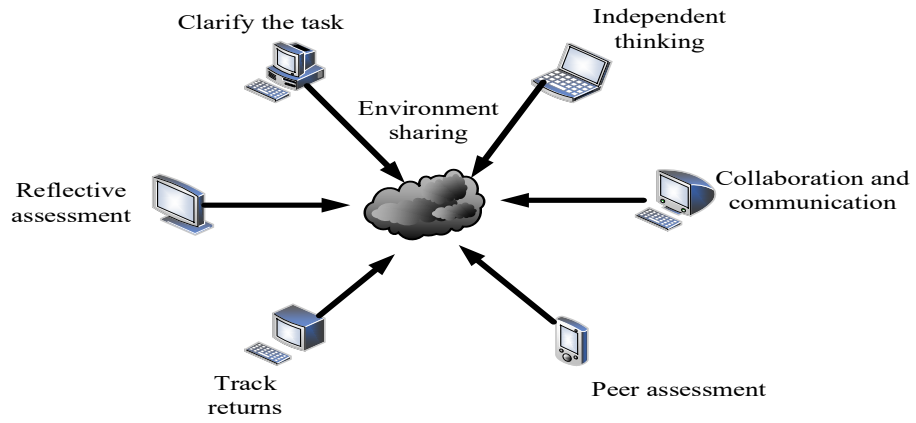

Figure 2: Learning activities of cloud computing-based educational resource sharing

The biggest feature of the visual computing platform for mathematics educational resources is resource sharing, sharing and mutual assistance. On this platform, users can speak freely, express their opinions, and share their information. The cloud computing platform is very suitable for data storage and collection, with large storage space and wide coverage, which significantly improves the utilization rate of resources by users and solves the problem of lack of educational resources in remote areas.

2.3 Image Denoising Methods

In image processing, since the image information is susceptible to external interference during the imaging process. Therefore, denoising is a necessary link in image processing. A typical image denoising method is shown in Figure 3:

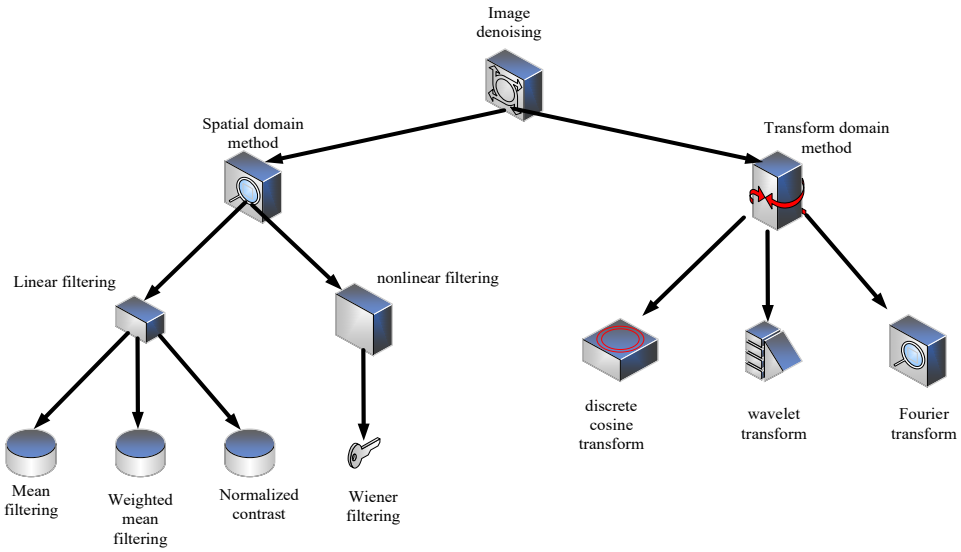

Figure 3: Typical image denoising method

These methods are used to analyze the denoising effect:

The image function filtered by the mean is represented as follows:

$$g(i,j) = \frac{1}{N}\sum_{(x,y\in M)} f(x,y) \tag{1}$$

A specific neighborhood is selected for weighted mean filtering, and the template is shown in formula 2:

ISSN 2616-5775 Vol. 7, Issue 5: 159-167, DOI: 10.25236/AJCIS.2024.070521

$$\frac{1}{16}\begin{bmatrix}1 & 2 & 1\\ 2 & 4 & 2\\ 1 & 2 & 1\end{bmatrix} \tag{2}$$

The central pixel gray value is replaced by the median value of all pixel arrangements in the area, namely:

$$g(i,j) = \mathrm{Med}\{f(x,y)\} \tag{3}$$

The total number of pixels on the image is N:

$$N = \sum_{i=0}^{T-1} N_i i \tag{4}$$

The probability is:

$$P_i = \frac{N_i}{n}, \sum_{i=0}^{T-1} P_i = 1 \tag{5}$$

The proportion of the target part to the image is:

$$\omega_0 = \sum_{i=0}^{t} p_i \omega_i = \sum_{t+1}^{T-1} p_i \tag{6}$$

The grayscale mean is:

$$\mu_0 = \sum_{i=0}^{t} i * \frac{p_i}{\omega_0} \mu_1 = \sum_{i=t+1}^{T-1} i * \frac{p_i}{\omega_1} \tag{7}$$

It's easy to get:

$$\mu = \omega_0 \mu_0 + \omega_1 \mu_1 \tag{8}$$

The between-class variance is:

$$g^2 = \omega_0(\mu_0 - \mu)^2 + \omega_1(\mu_1 - \mu)^2 = \omega_0\omega_1(\mu_0 - \mu_1)^2 \tag{9}$$

The mathematical form of the dilation operation can be expressed as:

$$A \oplus B = \left\{x \middle| \left[(\hat{B}) \cap A\right] \subseteq A\right\} \tag{10}$$

The mathematical form of the erosion algorithm can be expressed as:

$$A \ominus B = \{x | (B) \subseteq A\} \tag{11}$$

The co-occurrence matrix P is normalized:

$$p(i,j) = {}^{P(i,j)}/_{N} \tag{12}$$

The contrast is:

$$f_1 = \sum_i \sum_j |i - j^k| p(i,j) \tag{13}$$

The energy is:

$$f_2 = \sum_i \sum_j p(i,j) \tag{14}$$

The entropy is:

$$f_3 = -\sum_i \sum_j p(i,j) log_2 p(i,j) \tag{15}$$

In summary, the algorithm construction is completed.

2.4 Fast R-CNN Model Algorithm

The algorithm is refined by image denoising. The improved Fast R-CNN model algorithm proposes a multi-task loss function. The Fast R-CNN model algorithm is shown in Figure 4:

ISSN 2616-5775 Vol. 7, Issue 5: 159-167, DOI: 10.25236/AJCIS.2024.070521

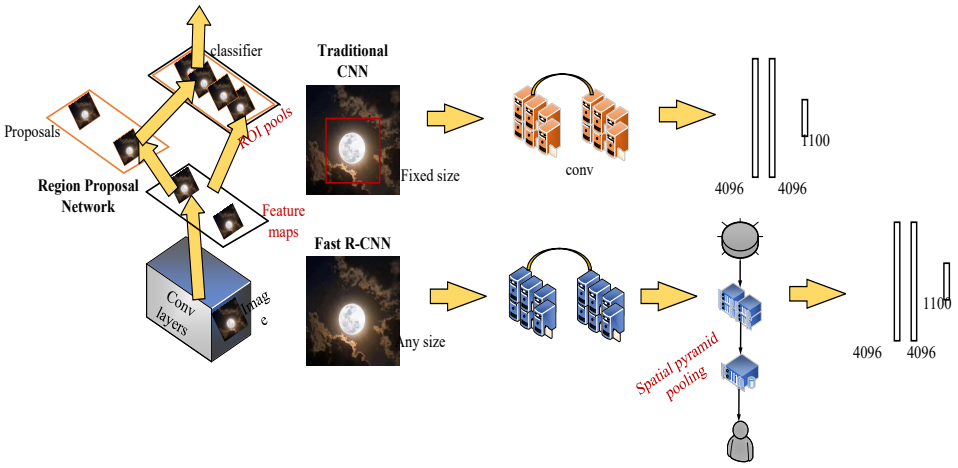

Figure 4: Fast R-CNN model algorithm

When testing the system, it is directly used to extract candidate regions. This greatly enhances the calculation speed, and finally meets the needs of the experiments in this paper.

2.5 Database Design

According to the analysis of system user requirements and the thinking of the function structure of the whole resource library, the main entities in this system are determined. As shown in Figure 5:

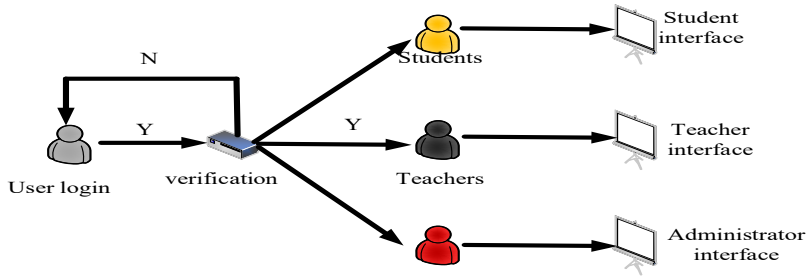

Figure 5: Database login design

3. Experiments on the Construction of a Visual Computing Model Platform for Mathematics Educational Resources

Due to the limitations of basic experimental conditions, when creating a distributed cluster, one computer is used as the main namenode server, and the other three computers are used as sub-servers. Through the relevant verification of the Linux environment, the data used in this test is 100g of mathematics teaching resources.

3.1 Comparison Test of Processing Speed with Different Number of Nodes

This test uses files of different sizes to test on one node and three nodes respectively, a total of six tests. The file size (MB) of each time is 9.4, 46.8, 93.7, 580.4, 1126.4, 2355.2, showing a state of increasing sequentially. The test results are shown in Figure 6:

ISSN 2616-5775 Vol. 7, Issue 5: 159-167, DOI: 10.25236/AJCIS.2024.070521

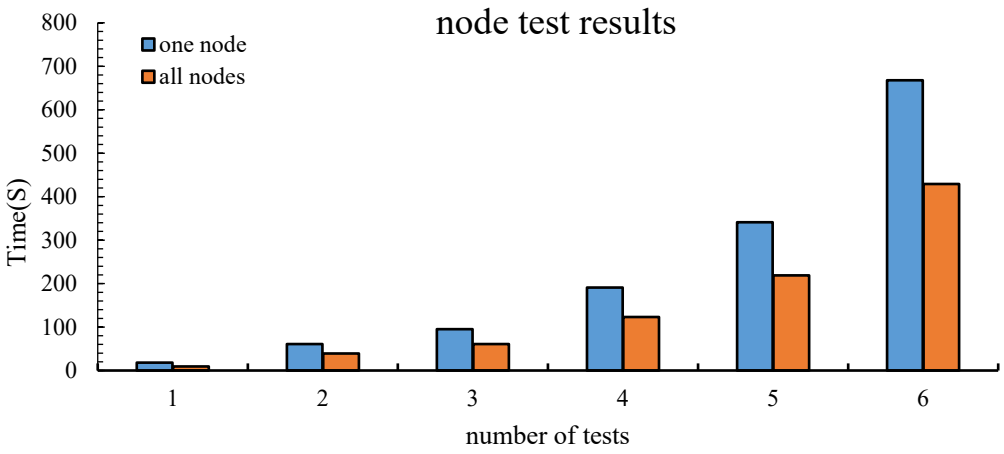

Figure 6: Node test results

As shown in the figure, it can be seen that when the first test is performed, the time used by one node is 8.6s longer than that of three nodes. In the sixth test, one node took 239s more time than three nodes. Three nodes process significantly faster than one node. As the number of files increases, the test effect is more obvious.

3.2 Performance Test of the Improved Fast R-CNN Model Algorithm

The data is divided into small, medium, and large groups according to size, and each group of data consists of two files of different sizes. Small group data is 199.4MB, 246.8MB. Medium data is 393.7MB, 580.4MB. Large data is 1126.4MB, 2355.2MB. The time-consuming comparison before and after improvement is used as the basis for performance testing. The small data set performance test results are shown in Figure 7:

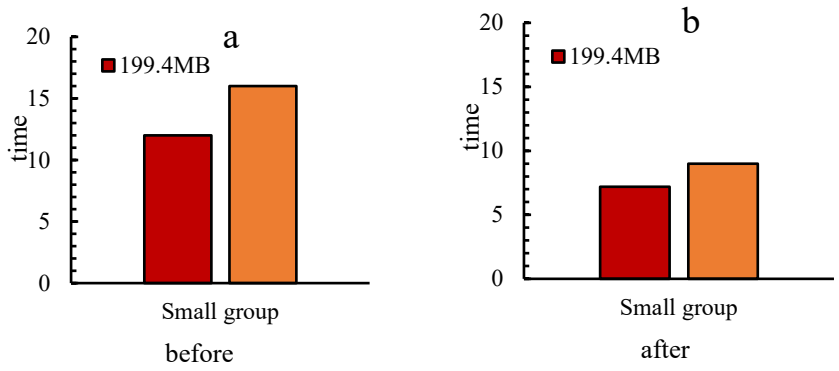

Figure 7: Small dataset performance test results

Figure 7(a) shows the response results of the test data before the algorithm is improved for the small data set. Figure 7(b) is the response results of the test data after the algorithm is improved for the small data set. Before the improvement, the 199.4MB data package took 12s, the 246.8MB data package took 16s, the improved 199.4MB data package took 7.2s, and the 246.8MB data package took 9s. Time is greatly shortened.

The performance test results of the medium data set are shown in Figure 8:

ISSN 2616-5775 Vol. 7, Issue 5: 159-167, DOI: 10.25236/AJCIS.2024.070521

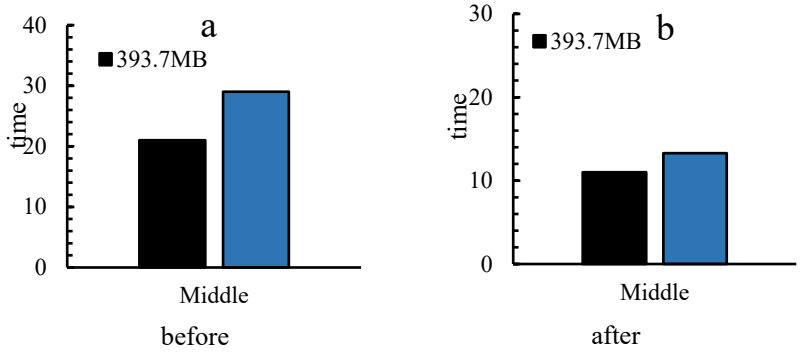

Figure 8: Medium dataset performance test results

Figure 8(a) shows the test data response results of the medium-sized data set before algorithm improvement, and Figure 8(b) shows the test data response results of the medium-sized data set after algorithm improvement. Before the improvement, the 393.7 data package took 21s, the 580.4MB data package took 29s, the 393.7MB data package after the improvement took 11s, and the 580.4MB data package took 13.3s. Time is further shortened.

The performance test results of large data sets are shown in Figure 9:

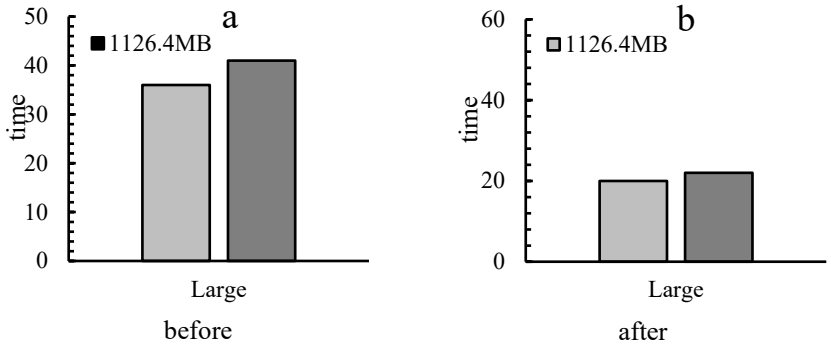

Figure 9: Large data set performance test results

Figure 9(a) shows the response result of the test data before the algorithm is improved for the large data set, and Figure 9(b) shows the response result of the test data after the algorithm improvement for the large data set. Before the improvement, the 1126.4MB data packet took 36s, the 2355.2MB data packet took 41s, and the 1126.4MB data packet took 20s after the improvement, and the 2355.2MB data packet took 22s. It shows that the access speed and data processing performance of the storage model can be improved by using this improved algorithm.

3.3 Depth Estimation in Image Processing

A circular area containing solid dots is selected as the sharpness evaluation area. Z_l and Z_r represent the depth of the left and right images, and the three-dimensional coordinates of the vertex center are shown in Table 1:

Table 1: 3D coordinates of vertex circle centers

	A	B	C	D
Z_l	98.2544	103.4787	121.1578	132.2474
Z_r	134.1457	146.9878	107.2345	119.6547

The least squares method is used to fit the 3D coordinates of the center of the circle in the sharpness evaluation area, and the results are shown in Table 2:

Table 2: Measurement results data

	a	b	c	Fitting variance
Left full focus plane	0.0572	0.0147	94.3174	6.2457
Right full focus plane	-0.0357	0.0245	137.2458	9.2458

ISSN 2616-5775 Vol. 7, Issue 5: 159-167, DOI: 10.25236/AJCIS.2024.070521

The coplanarity of 3D scatter points is evaluated using the variance estimated by plane fitting, and the estimated variances of plane fitting are 6.2457 and 9.2458, respectively.

The physical parameters of the LED array are shown in Table 3:

Table 3: Physical parameters of the LED array

Parameter	Index
Number of LEDs	16*16
IC model	WS2812
Voltage	DC 5V
electric current	2A
FPCB size	17cm*17cm*3cm
LED point distance	1cm
Single LED coverage angle	180

In this section, depth estimation in image processing is discussed, in particular by selecting a circular region containing solid points as the sharpness evaluation region. The least square method is used to fit the three-dimensional coordinates of the center of the circle, and the coplanarity of the three-dimensional scatter is evaluated by the variance estimated by the plane fitting. In addition, the physical parameters of the LED array are listed, which are essential for understanding how the entire system works.

4. Image Processing Using

4.1 Digital Image Processing Technology

Currently, the most common graphics formats on the Internet are image compression techniques that are used successfully. In order to adapt to efficient signal processing, many scholars are working on a new step in the development of chip technology, and this development trend is towards realizing the whole system in a single device. An FPGA includes design resources such as RAM, dedicated digital hardware, clock management, and transceivers. It has a built-in processing core.

4.2 Rough Classification of Image Processing Technology

Image filtering: Different image processing algorithms should be used to filter different kinds of noise to reduce the effect of noise on the overall image quality.

Image enhancement: The original archive image is converted into a digital archive image by converting input devices such as scanners, digital cameras, etc.

Image correction: Digital image processing often uses algorithms to change the position of pixels in an image.

5. Conclusions

The main contribution of this paper is to propose a visual computing model of mathematical educational resources combined with image processing technology, simplify the algorithm by HOG feature extraction and image denoising, and improves the Fast R-CNN model algorithm to improve the data processing speed and performance. In addition, a shared learning model based on cloud computing is constructed to enhance the visualization and spatial learning process of educational resources, thus improving students' mathematical critical thinking ability. Experiments verify the effectiveness of the proposed model and algorithm. Future research will focus on further optimizing the technology, expanding the application scope of the model, enhancing the user experience, and conducting cost-benefit analysis, while exploring interdisciplinary integration to achieve broader educational goals and deeper teaching outcomes.

References

[1] Amabili L, Gupta K, Raidou R G. A taxonomy-driven model for designing educational games in visualization. IEEE Computer Graphics and Applications, 2021, 41(6): 71-79.

ISSN 2616-5775 Vol. 7, Issue 5: 159-167, DOI: 10.25236/AJCIS.2024.070521

[2] Uranova V V, Bliznyak O V, Mazhitova M V, Isyakaeva R R. Role Of Visualization Of Educational Information In The Educational Process Of Medical And Biological Students In The "Analytical Chemistry" Discipline. Russian Journal of Education and Psychology, 2022, 13(6): 19-44.

[3] Zhang C, Liu X, et al. An Analysis on the Learning Rules of the Skip-Gram Model. 2019 International Joint Conference on Neural Networks, 2019, pp. 1-8

[4] Fatemah A, Rasool S, Habib U. Interactive 3D visualization of chemical structure diagrams embedded in text to aid spatial learning process of students. Journal of Chemical Education, 2020, 97(4): 992-1000.

[5] Ghamisi P, Maggiori E, Li S, Souza R, Tarablaka Y, Moser G, et al. New frontiers in spectral-spatial hyperspectral image classification: The latest advances based on mathematical morphology, Markov random fields, segmentation, sparse representation, and deep learning. IEEE geoscience and remote sensing magazine, 2018, 6(3): 10-43.

[6] Hsieh M C, Chen S H. Intelligence augmented reality tutoring system for mathematics teaching and learning. Journal of Internet Technology, 2019, 20(5): 1673-1681.

[7] Ruthotto L, Haber E. Deep neural networks motivated by partial differential equations. Journal of Mathematical Imaging and Vision, 2020, 62(3): 352-364.

[8] Hidayati D W, Kurniati L. The influence of self regulated learning to mathematics critical thinking ability on 3D-shapes geometry learning using geogebra. JIPM (Jurnal Ilmiah Pendidikan Matematika), 2018, 7(1): 40-48.

[9] Kishita Naoko. Distributed System Access Control for Fuzzy Mathematics and Probability Theory. Distributed Processing System, 2022, 3(3): 72-81.

[10] Rasti S, Bleakley C J, Holden N M. A Survey of High Resolution Image Processing Techniques for Cereal Crop Growth Monitoring. Information Processing in Agriculture, 2021, 7(50): 6-9.

[11] Keh A, Mp A. Crack Identification in Tungsten Carbide Using Image Processing Techniques. Procedia Structural Integrity, 2022, 37(2): 274-281.

[12] Sm A, Mvk B, Sjjt C. Vehicle damage protection using sensors using image processing techniques. Materials Today: Proceedings, 2021, 7(8): 9-10.

[13] Hou Y, Li Q, Zhang C. The State-of-the-Art Review on Applications of Intrusive Sensing, Image Processing Techniques, and Machine Learning Methods in Pavement Monitoring and Analysis. Engineering, 2020, 7(3):89-92.

[14] Rkvp A, Sg A, Hkb B. A Novel Method for Indian Vehicle Registration Number Plate Detection and Recognition using Image Processing Techniques. Procedia Computer Science, 2020, 167(2): 2623-2633.

[15] Salvi M, Acharya U R, Molinari F. The impact of pre- and post-image processing techniques on deep learning frameworks: A comprehensive review for digital pathology image analysis. Computers in Biology and Medicine, 2020, 128(2): 104-129.